Phase-Sensitive Near-Field Measurements and Electromagnetic Simulations of a Double-Slot HEB Integrated Lens-Antenna Mixer at 1.1, 1.2 and 1.6 THz

Willem Jellema, Timothy J. Finn, Andrey Baryshev, Maarten van der Vorst, Stafford Withington, *Member, IEEE*, J. Anthony Murphy, *Member, IEEE* and Wolfgang Wild

***Abstract*—The application of integrated lens-antennas becomes increasingly important as submillimetre-wave mixer and detector research moves towards frequencies well above 1 THz. Although classical waveguide receivers seem feasible up to 2.5 THz, planar integrated-antenna technology offers clear advantages when losses, manufacturing, integration, and the fabrication of large-format imaging arrays are considered. Modeling of planar antennas in combination with dielectric lenses has been reported by Filipovic and van der Vorst [1, 2]. Their simulations are based on a hybrid geometrical/physical optics (GO/PO) model, which predicts, mainly, far-field radiation patterns. This approach, as implemented in the software package PILRAP, has, for example, been used to design the lens antennas of the quasi-optical mixers used in the Heterodyne Instrument for the Far-Infrared (HIFI). In this paper we present measurements and simulations of a HEB double-slot lens-antenna mixer as present in Band 6L of HIFI. Amplitude and phase measurements were taken at 1.1, 1.2 and 1.6 THz respectively. We provide a detailed description of the experimental technique, which offers phase-sensitive measurements up to 1.6 THz with a dynamic range as high as 80 dB. We also describe comparisons between PILRAP simulations and experimental data. Understanding the precise radiation patterns of these devices is essential because once they are coupled to optical systems, their near-field behavior can influence the performance of the overall instrument considerably. We furthermore discuss to what extent the theory and experiment agree, and identify the key difficulties when modeling fast lens-antennas, particularly the problems associated with modeling the near-field. We conclude by outlining a few ideas as to how it might be possible to model these systems through the use of commercial planar antenna simulators, and new electromagnetic propagation techniques.**

***Index Terms*—Integrated lens-antenna, phase-sensitive, near-field, THz beam measurements.**

Manuscript received May 31, 2005. This work was supported in part by Enterprise Ireland (Prodex), the Science Foundation Ireland (SFI), and in part by the National University of Ireland, Maynooth.

Willem Jellema is with the National Institute for Space Research of the Netherlands (SRON) and the Kapteyn Astronomical Institute, University of Groningen, P.O. Box 800, 9700 AV Groningen, the Netherlands (phone: +31-50-363-4058; fax: +31-50-363-4033; e-mail: W.Jellema@sron.nl).

Timothy J. Finn and J. Anthony Murphy are with the National University of Ireland, Maynooth, Co. Kildare, Ireland.

Andrey Baryshev and Wolfgang Wild are with the National Institute for Space Research of the Netherlands (SRON) and the Kapteyn Astronomical Institute, University of Groningen, P.O. Box 800, 9700 AV Groningen.

Maarten van der Vorst is with the European Space Agency, ESTEC, P.O. Box 229, 2200 AG Noordwijk, the Netherlands.

Stafford Withington is with the Cavendish Laboratory, Madingley Road, Cambridge CB3 0HE, United Kingdom.

I. Introduction

THE use of waveguide feedhorns in submillimeter-wave optical systems is widely established and the electromagnetic properties of these systems are well validated [3, 4]. The application of waveguide feedhorns seems feasible up to 2.5 THz but is mechanically becoming difficult beyond 1.5 THz. At these frequencies planar integrated lens-antennas start to offer manufacturing advantages. Pioneering work in the area of modeling the radiation patterns of planar-integrated lens-antenna systems was carried out by Filipovic and van der Vorst [1, 2]. Their hybrid geometrical/physical optics model (GO/PO) has been verified experimentally mainly in far-field amplitude at frequencies below 1 THz. The implementation of this modeling technique in the software package PILRAP was used for the quasi-optical design of the lens-antenna mixers in band 5, 6L and 6H of the Heterodyne Instrument for the Far-Infrared (HIFI) [5, 6]. Due to mass and volume constraints in HIFI the optical layout around the lens-antenna system is relatively compact. Consequently the mirrors are located in the propagating near-field of the lens-antenna. In [3] and [4] it is shown that the near-field characteristics of such systems can be very important for the overall optical performance of the instrument.

In this paper we report experimental results obtained for a number of lens-antenna geometries at 1.1, 1.2 and 1.6 THz. In addition to the measurement of field amplitudes the presented experimental system is capable of measuring the phase distributions directly. This opens up the possibility to verify the near-field properties of lens-antenna systems and to validate the predicted phase-centers by PILRAP at frequencies beyond 1 THz. Our primary objective in this work is to verify the predicted first-order beam properties: the waist size of the fundamental Gauss-Laguerre mode and the position of its

phase-center relative to the lens geometry. As a secondary objective we will address the question to what extent electromagnetic simulations based on PILRAP and GRASP and phase-sensitive beam measurements of optical systems employing lens-antenna systems agree.

II. Experimental Setup

A. Receiver and Scanner System

The experimental system is based on using an HEB mixer device in the heterodyne detection mode. The HEB mixer device is coupled via a double-slot antenna on a silicon lens to free-space or the optical system. The Local Oscillator (LO) as well as the RF test source are based on a solid-state multiplier chain driven by W-band power amplifiers. The input W-band synthesizers are based on high spectral purity low phase noise X-band synthesizers and Spacek active multiplier chains (sextuplers). The overall diagram for the 1.6 THz configuration is shown in Fig. 1. Two synthesizers S_1 and S_2 drive the RF resp. LO chain. The RF test source is mounted on a mechanical scanner that can move in x, y and z. By scanning the RF test source on a plane in front of the lens-antenna system with HEB mixer, the spatial coupling between the small RF test source probe and the lens-antenna system under test can be mapped. The measured complex coupling coefficient is proportional to the radiated field of the lens-antenna system if it would have been used as a transmitter. The total LO and RF multiplication factor is 108 in this case. To construct a reference signal against which the relative amplitude and phase of the HEB mixer signal can be measured, a fraction of the signal of the two synthesizers is mixed to low frequency (<100 MHz) and multiplied by the same amount as in the LO and RF chain. The obtained reference signal is fully correlated in phase to that of the HEB mixer but has fixed amplitude as a saturated reference multiplier system is used. In Fig. 1. the reference signal is denoted by R and the detected signal (modulated by spatial movement of the scanner) is denoted by S.

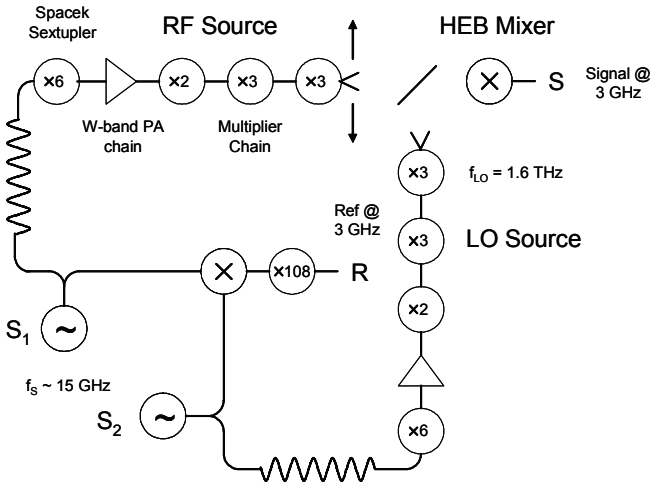

Fig. 1. Diagram of phase-sensitive measurement system at 1.6 THz.

B. Compensation of Correlated Phase Variations

Because of the high multiplication factor the phase variations of the two synthesizers are multiplied by a significant amount. In order to allow for narrow-band detection we first compensate the correlated variations in R and S by the system shown in Fig. 2. The system is based on a standard network S_{21} network parameter measurement using a Vector Network Analyzer (VNA) in CW mode. The test signal transmitted on port 1 of the VNA is first mixed with R to low frequency. This intermediate signal is filtered, amplified and finally drives a second mixer in which the correlated variations of R and S are added in anti-phase. In this process the phase information, i.e. the phase difference between R and S, is conserved whereas the signal power is no longer scattered over a relatively large bandwidth. In practice it is possible to measure in a bandwidth as narrow as 10 Hz yielding a very high signal-to-noise ratio up to 90 dB at 1.6 THz.

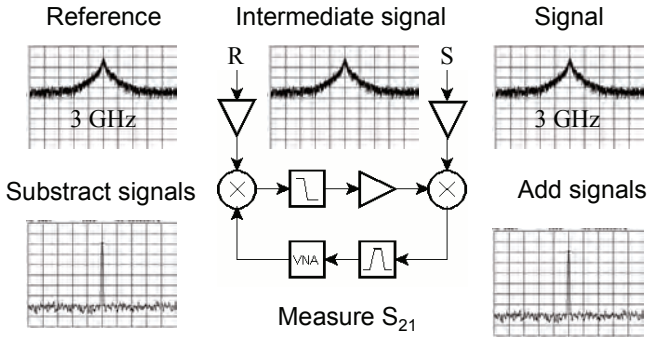

Fig. 2. Compensation of correlated phase variations in the reference and detected signal R resp. S.

C. Sensitivity and Dynamic Range

The noise temperature T_N of the HEB mixer in our experiment at 1.6 THz is typically 2000 K. We estimate an available RF test signal power P_s of order of 10 nW. The coupling efficiency η between test signal probe and lens antenna system under test in this particular case is of order of -20 dB. When an IF bandwidth B of 100 Hz is taken and an integration time τ of 0.26 s the signal-to-noise ratio SNR can be calculated using the radiometer equation[7]:

$$SNR \sim \frac{\eta P_s}{kT_N}\sqrt{\frac{\tau}{B}} \qquad (1)$$

At 1.6 THz the expected SNR is of order of 80 dB which is in very good agreement with the actual measured value.

D. First-order Standing Wave Correction

Another important feature of our experimental setup is the correction of standing waves between RF test probe and lens-antenna system under test. Because phase is directly measured

with high signal to noise a first-order standing wave correction can easily be made. If we denote the complex coupling coefficient between probe and antenna by c the measured signal s can be expressed as follows:

$$s \propto c\left(1+\sum_{n=1}^{\infty} R^n |c|^{2n} e^{-i\frac{4\pi nL}{\lambda}}\right) \qquad (2)$$

In deriving (2) it is assumed that the dominant reflections occur at the multiplier and mixer device. We furthermore assume that the reflected fields have the same first-order Gaussian beam characteristics and couple with equal efficiency for each roundtrip order. The roundtrip reflection coefficient is denoted by R. Each next roundtrip contribution to the measured signal s drops in amplitude by the product of the roundtrip reflection and squared magnitude of the coupling. Each subsequent roundtrip contribution is however modulated in phase by a plane-wave phase shift corresponding to the roundtrip pathlength 2L between the devices.

The first-order standing wave correction that can be made is based on measuring the signals s_1 and s_2 in two planes separated by λ/4. From (2) it can be seen that the phase of the first roundtrip term therefore changes by π. If the beam is reasonably well collimated the first-order effect on the measured coupling is only a plane-wave phase shift of π/2. Ignoring roundtrip terms beyond n = 1 the following relation for the compensated signal s_c can be found which provides a first-order correction for standing waves:

$$s_c = \frac{s_1 + s_2 e^{i\frac{\pi}{2}}}{2} \approx c \qquad (3)$$

In our system we use the z-stage of the xyz-scanner to measure a two-dimensional grid of pairs of points separated in z by λ/4. An on-axis scan in z has shown that when using (3) the standing wave ripple can be reduced by almost an order of magnitude and the residual standing wave ripple can be as low as 0.05 dB in the main beam.

E. Alignment between Scanner and Lens-Antenna System

The absolute alignment between the scanner system and the lens-antenna system under test is established by using two pairs of alignment devices. Two reflecting mirrors are mounted left and right of the optical axis of the lens-antenna system (see Fig. 3). The normal vectors of the mirror surfaces are parallel to the optical axis within a few arcmin. On the mirror surfaces we have machined crosshairs by using a 20 µm diamond dicing saw. The centers of the crosshairs are measured with respect to the optical axis by means of an optical traveling microscope. On the scanner system two plan-parallel alignment windows are mounted left and right of the test signal probe. Again the normal vectors of the windows are nearly normal to the scan plane and the centers of the crosshairs are accurately known with respect to the horn aperture. The orientation of the scan plane is first aligned with respect to the optical axis by auto-collimating on an alignment mirror and window pair using an optical theodolite. When the scan plane is normal to the optical axis the x- and y-stages of the scanner are used to align the crosshairs on the alignment mirror and window. The rotation of the x- and y-axis of the scanner in the plane of measurement is finally determined by measuring the x- and y-offsets between the crosshair centers on the other pair of alignment devices. The alignment accuracy is typically 0.1 mm in lateral position and within a few arcmin for tilt. Rotation in the measurement plane is known as accurate as 0.1 deg and the axial location of the scan plane is determined within 1 or 2 mm. The absolute coordinates of the measured field data is therefore known within fractions of a wavelength.

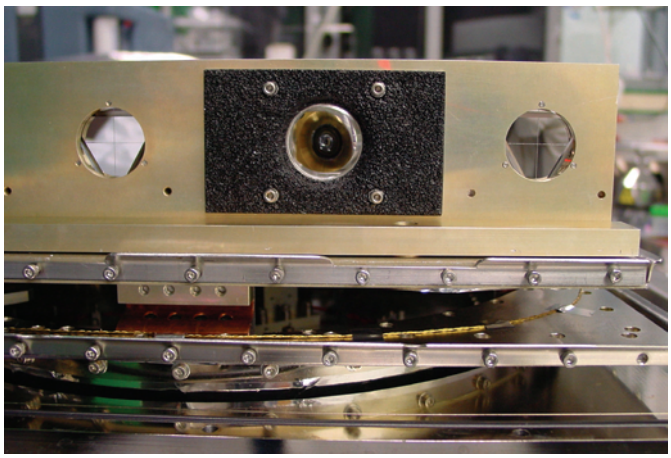

Fig. 3. Alignment mirrors left and right of the optical axis. The silicon lens of the lens-antenna system is visible in the optical port surrounded by a SiC absorber panel.

F. Phase Stability and Drift Correction

Direct measurement of phase at 1.6 THz requires very good mechanical and thermal stability to reduce phase errors as far as possible. We therefore use special phase-stable cables from Reynolds. The differential thermal expansion coefficient of the dielectric material used in this cable is nearly zero at room temperature. By using identical cables between S_1 and S_2 and the RF and LO sources in Fig. 1. the thermal drift problem is furthermore reduced to differential thermal drift. When mapping the 2-dimensional field we take a calibration measurement at a fixed point in space after each line scan. As all data is time-stamped the final data can be corrected for drift by linear interpolation of the calibration trace [8]. The typical drift is 20 to 30º per hour, but the residual error after correction is smaller than 5º. The phase error due to the flexing cable of the RF test source is characterized by measuring the roundtrip phase delay along the cable over the scan plane with a VNA. The maximum phase excursion over the scan plane is kept within 10º by fixing the cable in a constant bending radius.

G. Summary Measurement Accuracy and Performance

In the previous sections we have outlined the key characteristics and unique features of the experimental setup. Novel is the capability of measuring phase at 1.1, 1.2 and 1.6 THz with demonstrated dynamic range of 70, 70 resp. 80 dB in a 100 Hz IF bandwidth. We have presented a system that compensates correlated phase variations allowing for unlimited narrow-band measurements. Furthermore standing wave errors are corrected for to first-order by taking measurements in two planes separated by λ/4. The measurement geometry is mechanically controlled within fractions of a wavelength and the phase stability of the system is excellent because of the symmetric arrangement of special phase-stable cables.

The overall measurement accuracy is better than 20º in phase and 0.5 dB in amplitude in the main beam (above the -20 dB level). For a detailed example of performance characterization and error analysis and demonstration of measurement capability at 480 GHz we refer the reader to [4] and [8].

III. Test Cases

In this paper we consider the lens-antenna design depicted in Fig. 4. The lens-antenna system consists of an elliptical lens of 5 mm diameter. The major axis, along the optical axis, is denoted by a and the minor axis, the lens radius, is denoted by b. In a number of cases a Parylene anti-reflection coating of 28 μm is applied. The lens body is extended by a Silicon cylinder. The total Silicon extension length is denoted by L and is composed of the substrate thickness of the HEB chip and the cylindrical lens extension.

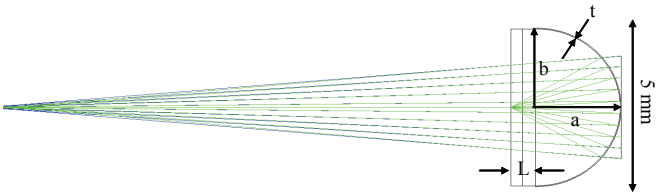

Fig. 4. Optimized elliptical lens design for HIFI Band 6L.

The design values for a and b are 2.548 resp. 2.500 mm and the extension length is designed to be 0.756 mm. The double-slot antenna for Band 6L of HIFI has a slot width of 4 μm, a slot length of 56 μm and a slot separation of 32 μm. For these parameters PILRAP predicts a waist size for the fundamental Gauss-Laguerre mode of 0.57 mm @ 1.6 THz which is located at 18.6 mm behind the lens vertex. The lens design is relatively sensitive to manufacturing tolerances. A change of 10 μm in the extension length changes the waist size roughly by 10% whereas the phase center moves by about 1 mm. Therefore the actual lens-geometry measured should be known within a few μm. For that purpose we designed a special mechanical bracket for the Silicon lens as shown in Fig. 5. At an external mechanical calibration facility the lens surface and flange planes were mechanically sampled in one run using a 0.3 mm radius diamond probe with a contact force of 5 mN applied normal to the surface. The total number of about 50 points was then fitted to an elliptical surface in a three-dimensional coordinate system.

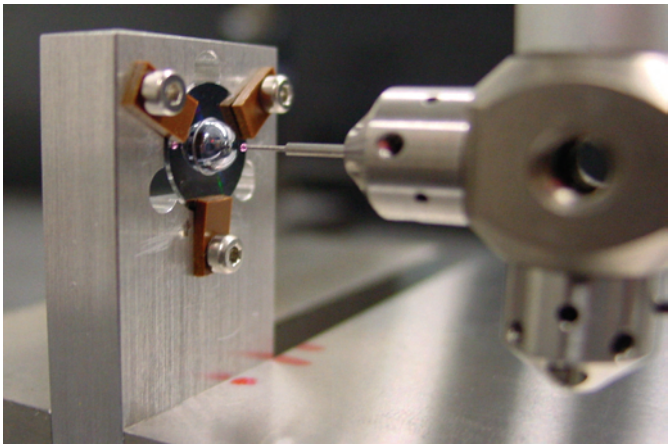

Fig. 5. Mechanical characterization of lens-antenna geometry.

The measurement accuracy of this method is about 2 μm. Although the lenses were ordered from the same company on the basis of the same drawing a large spread in lens geometry was found. As a result the expected spread in F/D ratio ranges from 3.2 to 4.8. Not only deviations in extension length were found but also deviations in ellipticity. The four test cases that are considered in this paper are summarized in Table I.

TABLE I
SUMMARY TEST CASE CHARACTERISTICS

Case	AR coating	a (mm)	b (mm)	ellipticity	L (mm)
SRON[a]	no	2.546	2.499	1.0191	0.758
FM01[b]	yes	2.516	2.501	1.0060	0.771
FM04[b]	yes	2.529	2.496	1.0134	0.726
DM3[b]	no	2.537	2.499	1.0147	0.767

[a]Lens-antenna system and HEB device from SRON-DIMES
[b]Lens-antenna system and HEB devices from CTH

IV. Measurement and Modelling Results

A. SRON lens-antenna system at 1.1 and 1.3 THz

The first measurements are taken at 1.1 and 1.3 THz for the SRON lens (first case in Table I). This lens geometry was very close to the designed case. No AR coating was used for this experiment. In Fig. 6. the measured phase distribution is plotted clearly demonstrating our capability of measuring phase at THz frequencies. Note that at the right of Fig. 6. the frame of the beamsplitter can be recognized although the intensity has dropped already by 45 dB. By Fourier-transforming the near-field data to the far-field a direct comparison between PILRAP and the measurement can be made. The predicted and measured far-field H-plane distribution is shown in Fig. 7 together with the fundamental Gaussian beam providing highest coupling efficiency [9].

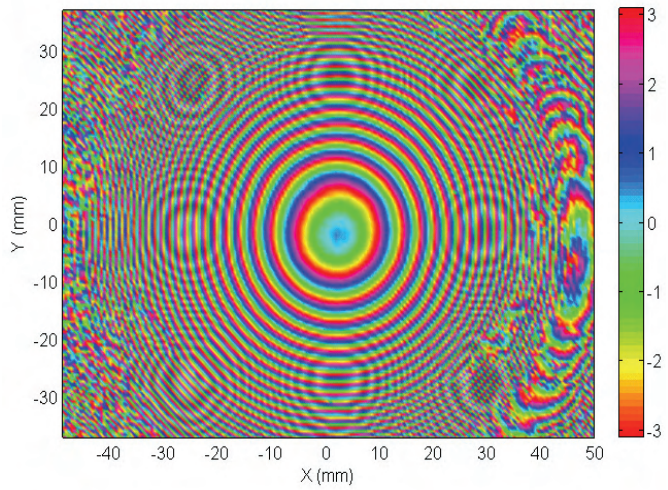

Fig. 6. Measured phase distribution for SRON lens at 1.1 THz.

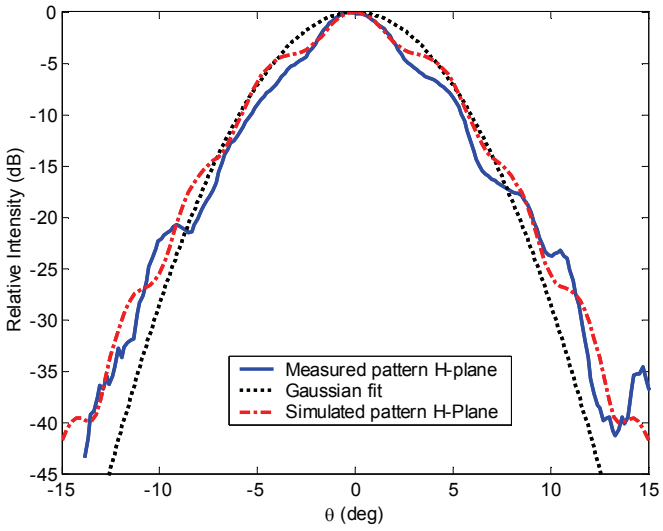

Fig. 7. Predicted and measured H-plane far-field distribution and fundamental Gaussian beam yielding highest coupling for the SRON lens at 1.1 THz

The predicted waist size at 1.1 THz is 0.66 mm whereas we measure 0.67 mm. For the phase center location we measure a value of -(15±2) mm whereas PILRAP predicts -15.7. The measured gaussicity is 92% whereas PILRAP predicts 95%. Within the measurement uncertainties this is all in very good agreement regarding first-order beam properties. Similar agreement is found at 1.2 THz. When looking to the sidelobe structure in Fig. 7. it can be seen that the main beam agrees reasonably well in the upper 5 dB. Below that, the sidelobe structure is different. In the E-plane we find even larger deviations, but also significant asymmetry in the sidelobe structure. The E-plane asymmetry could be chip- or antenna-related as PILRAP only simulates two isolated slots and does not take into account the asymmetrically coupled IF line and RF choke. We conclude that although the first-order properties are reasonably well predicted the measured and predicted sidelobe structure at lower intensity levels is not quite the same.

B. CTH lens-antenna systems at 1.6 THz

In order to achieve more measurement resolution for the phase center position the lenses FM01, FM04 and DM3 listed in Table I are integrated into the Mixer-Sub Assembly (MSA) optics for band 6L. This system images the front of the lens via a three-mirror system to a pupil plane of the Focal Plane Unit (FPU) of HIFI [3-6]. At the output of the MSA the Gaussian beam width is about 3.55 mm and relatively collimated. A measurement accuracy in the axial position of 2 mm at the output corresponds to an accuracy of about 0.1 mm at the input near the lens-antenna system. Assuming the optics are perfectly shaped and well-aligned, the Gaussian beam parameters found at the output plane can be back-traced to the input using the ABCD matrix method for the complex beam parameter [9]. In that way the position of the phase center of the lens-antenna system can be accurately determined by making use of the optical magnification of the MSA optics.

In Fig. 8. the measured and simulated phase distribution for lens DM3 at 1.6 THz at the output of the MSA optics is shown. The simulation is done by using a GRASP model of the MSA optics and the input field predicted by PILRAP.

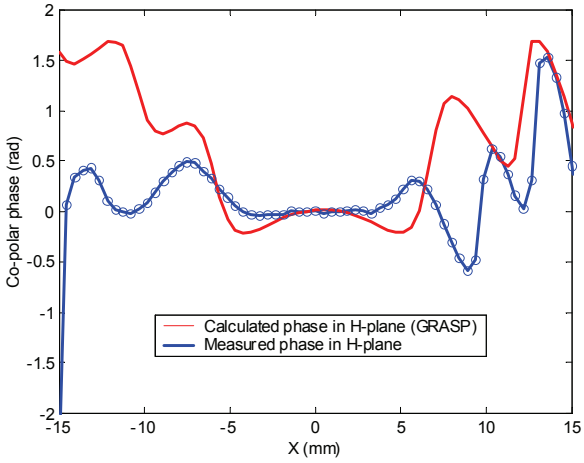

Fig. 8. GRASP8 simulation of MSA optics including lens DM3 at 1.6 THz.

Clearly visible is the difference in phase curvature. Note that the field is only significant in the range between -7 and +7 mm where more than 99% of the power is concentrated. In this particular case the defocus between measured and predicted waist location is 75 mm. The measured and predicted waist sizes are however in good agreement at about 3.6 mm. Using the ABCD matrix method for the complex beam parameter the Gaussian beam parameters at the lens-antenna are retrieved. The results for the retrieved lens-antenna waist size and phase center are summarized in Fig. 9. for lenses DM3, FM01 and FM04 together with the predicted values by PILRAP. The lens-geometry for DM3 is reasonably close to the designed case. The PILRAP simulation for this case is taken as the reference, hence a defocus of 0 mm by definition. Comparing the measured and simulated parameters one can see that in all cases the waist size is in good agreement but the phase center is systematically closer to the lens vertex. The offset

furthermore scales with waist size and is +1.5 mm for DM3, +0.7 mm for FM01 and +0.3 for FM04. The observed offsets in phase center are significant, about 20 to 30% of the confocal distance, and significantly larger than the measurement error of about 0.1 mm. We conclude therefore that PILRAP does not correctly predict the phase-center for this particular lens-antenna design.

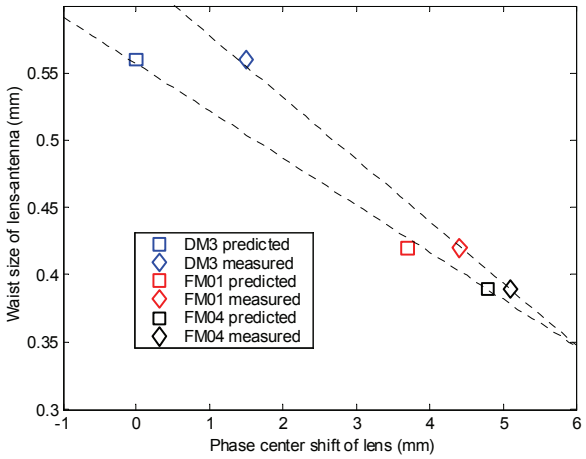

Fig. 9. Measured and predicted lens-antenna waist size and location.

V. Summary And Conclusions

In this paper we have demonstrated phase-sensitive beam pattern measurements of twin-slot HEB lens-antenna mixers at 1.1, 1.2 and 1.6 THz with signal-to-noise ratios ranging from 70 to 80 dB in a 100 Hz bandwidth. We used this system to measure a number of well-known lens-antenna geometries and compared measured beam parameters with those predicted by PILRAP. We found that the measured first-order Gaussian beam widths agree within a few percent with predicted values from PILRAP. The predicted beam patterns agree in general fairly well in the main beam. The H-plane cuts show best agreement, but sidelobe structure is not correctly predicted. In the E-plane we see in general asymmetry which might be chip- or antenna-related. For this particular lens-antenna design our main conclusion is however that the measured phase center appears systematically closer to the lens vertex than predicted by PILRAP. The offset scales furthermore with waist size.

We believe that this experimental investigation addresses for the first time the validation of the predicted phase-center location by PILRAP at frequencies beyond 1 THz. These results invite for independent verification and progress in lens-antenna modeling. Key difficulties for this design might be the relatively short radius of curvature of the lens surface, the position of the lens surface at about 6 confocal distances of the feed pattern, feedback of internal reflections and reflected back-radiation on the current distribution of the double-slot antenna and chip details not considered in PILRAP, e.g. the finite size of the substrate, presence IF line and RF choke and glue layer between chip and lens. We first propose to independently verify the first-order and large-scale effects by a hybrid model combining the strengths of commercial planar antenna simulation packages and a near-field propagation technique scattering a set of incoming polarized plane waves from the antenna through the lens surface by using a Singular Value Decomposition (SVD) technique. As a second step the remaining difficulties, that most likely show up in details of the sidelobe structure, might be addressed through the use of Finite Difference Time Domain (FDTD) techniques.

Acknowledgment

The authors would like to thank Sergey Cherednichenko and Therese Berg from Chalmers University of Technology (CTH), Göteborg, Sweden for providing the lens-antenna HEB mixers used at 1.6 THz. We are furthermore grateful to Merlijn Hajenius and Jianrong Gao from the Kavli Institute of NanoScience Delft, Delft University of Technology, the Netherlands for their work on the HEB lens-antenna mixer used at 1.1 and 1.2 THz. At the National Institute of Space Research of the Netherlands we acknowledge Jochem Baselmans, Pieter Dieleman, Marinus Jochemsen, Martin Eggens and Geert Keizer for their help in taking measurements. We also acknowledge Tully Peacocke and John Lavelle at the National University of Ireland, Maynooth for running PILRAP and GRASP simulations. Finally special thanks to John Ward and John Pearson from Jet Propulsion Laboratory, Pasadena, USA for loaning us the 1.6 THz LO and RF test source as well as test hardware for the 1.1 and 1.2 THz RF test source without which we would not have been able to do these measurements.

References

[1] D. F. Filipovic, S. S. Gearhart and G. M. Rebeiz, "Double-slot Antennas on Extended Hemispherical and Elliptical Silicon Dielectric Lenses", *IEEE Trans. Microwave Theory Tech.*, Vol. 41, 1993, pp. 1738-1749.

[2] M .J. M. van der Vorst, "Integrated Lens Antennas for Submillimetre-wave Applications", Ph.D. dissertation, Eindhoven University of Technology, the Netherlands, 1999.

[3] W. Jellema et al , "Experimental Verification of Electromagnetic Simulations of a HIFI Mixer Sub-Assembly", *Proc. 14th Int. Symp. on Space Terahertz Technology*, Tucson, USA, April 22-24, 2003.

[4] W. Jellema, R. Huisman, N. Trappe, T. J. Finn, S. Withington and J. A. Murphy, "Comparison of Near-Field Measurements and Electromagnetic Simulations of the Focal Plane Unit of the Heterodyne Instrument for the Far-Infrared" et al, *Proceedings of the 5th Int. Conf. on Space Optics*, Toulouse, France, March 30 – April 2, 2004.

[5] B. D. Jackson, "NbTiN-Based THz SIS Mixers for the Herschel Space Observatory", Ph.D. dissertation, University of Groningen, National Institute for Space Research of the Netherlands and the Delft University of Technology, all in the Netherlands, 2005, Chapter 7, pp. 147-176.

[6] B. D. Jackson, K. J. Wildeman and N. D. Whyborn on behalf of the HIFI consortium, "The HIFI Focal Plane Unit", *Proc. 13th Int. Symp. on Space Terahertz Technology*, Cambridge, USA, 26-28 March 2002, pp. 339-348.

[7] J. Lesurf, *Millimeter-wave Optics, Devices & Systems*, Adam Hilger: Bristol and New York, 1990, pp. 113.

[8] W. Jellema et al, "Performance Characterisation and Measurement Results of a Submillimeter-Wave Near-Field Facility for the Heterodyne Instrument for the Far-Infrared", *Proc. 3rd ESA Workshop on Millimeter Wave Technology and Applications*, Espoo, Finland, May 21-23, 2003.

[9] P. F. Goldsmith, *Quasioptical Systems: Gaussian Beam Quasioptical Propagation and Applications*, IEEE Press:New York, 1997, Chapter 3 and 7.